Influence of mesoscale eddies on the distribution of nitrous oxide in the eastern tropical South Pacific

D. L. Arévalo-Martínez[1], A. Kock[1], C. R. Löscher[2], R. A. Schmitz[2], L. Stramma[1], and H. W. Bange[1]

[1] {GEOMAR Helmholtz Centre for Ocean Research Kiel, Düsternbrooker Weg 20, 24105 Kiel, Germany}

[2] {Institute of Microbiology, Christian Albrechts University of Kiel, Am Botanischen Garten 1-9, 24118 Kiel, Germany}

Correspondence to: D. L. Arévalo-Martínez (darevalo@geomar.de)

Short title: Mesoscale eddies and N_2O in the ETSP

Abstract

Recent observations in the eastern tropical South Pacific (ETSP) have shown the key role of meso- and submesoscale processes (e.g. eddies) in shaping its hydrographic and biogeochemical properties. Off Peru, elevated primary production from coastal upwelling in combination with sluggish ventilation of subsurface waters fuels a prominent oxygen minimum zone (OMZ). Given that nitrous oxide (N_2O) production/consumption processes on the water column are sensitive to oxygen (O_2) concentrations, the ETSP is a region of particular interest to investigate its source-sink dynamics. To date, no detailed surveys linking mesoscale processes and N_2O distributions as well as their relevance to nitrogen (N) cycling are available. In this study, we present the first measurements of N_2O across three mesoscale eddies (two mode water or anticyclonic and one cyclonic) which were identified, tracked and sampled during two surveys carried out in the ETSP in November-December 2012. A two-peak structure was observed for N_2O, wherein the two maxima coincide with the upper and lower boundaries of the OMZ, indicating active nitrification and partial denitrification. This was further supported by the abundances of the key gene for nitrification *amoA* and the gene marker for N_2O production during denitrification, *nirS*. Conversely, we found strong N_2O depletion in the core of the OMZ (O_2 < 5 μmol L^{-1}) to be consistent with nitrite (NO_2^-) accumulation and low levels of nitrate (NO_3^-), thus suggesting active denitrification. N_2O depletion within the OMZ's core was substantially higher in the center of mode water eddies, supporting the view that eddy activity enhances N-loss processes off Peru, in particular near the shelf break where nutrient-rich, productive waters from upwelling are trapped before being transported offshore. Analysis of eddies during their propagation towards the open ocean showed that, in general, "aging" of mesoscale eddies tends to decrease N_2O concentrations through the water column in response to reduced supply of material to fuel N-loss, although hydrographic variability might also significantly impact the pace of the production/consumption pathways for N_2O. Our results evidence the relevance of mode water eddies for N_2O distribution, thereby improving our understanding of the N-cycling processes, which are of crucial importance in times of climate change and ocean deoxygenation.

1 Introduction

Nitrous oxide (N_2O) is an atmospheric trace gas which strongly affects Earth's climate both by contributing to the greenhouse effect and by its role as a major ozone-depleting substance (Ravishankara et al., 2009; Myhre et al., 2013). The ocean is a net source of N_2O to the atmosphere accounting for about one third of the total natural source (Myhre et al., 2013), and therefore, the investigation of its formation pathways under changing oceanic regimes is relevant for any future predictions of how the nitrogen (N) cycle will react to future climate change. N_2O is mainly produced by microbial nitrification and denitrification, with particularly high yields under low oxygen (O_2) conditions (Goreau et al., 1980; Naqvi et al., 2010; Löscher et al., 2012; Bakker et al., 2014) such as those found in oxygen minimum zones (OMZ) of the tropical oceans. In the eastern tropical South Pacific (ETSP) a prominent OMZ is formed and maintained by the close coupling between elevated primary production fueled by coastal upwelling and weak ventilation of intermediate waters (Karstensen et al., 2008). Hence, elevated production of N_2O in subsurface low-O_2 waters in conjunction with their transport towards the surface make the ETSP a "hotspot" for emissions of this climate-relevant gas to the atmosphere (Arévalo-Martínez et al., 2015). However, even though N_2O production in low-O_2 waters could supply as much as 25% – 50% of the global ocean source (Suntharalingam et al., 2000), it has been shown that when O_2 concentrations fall below about 5 µmol L^{-1} (in the OMZ's core) N_2O consumption through denitrification ($NO_3^- \rightarrow NO_2^- \rightarrow NO \rightarrow N_2O \rightarrow N_2$) takes place, and therefore these waters may act as a net sink for this gas (Codispoti and Christensen, 1985; Löscher et al., 2015b). Hence, OMZ's have a significant role in the marine N cycle not only due to their influence on the subsurface production of climate relevant trace gases such as N_2O (Paulmier et al., 2008; Codispoti, 2010; Capone and Hutchins, 2013) but also because of their contribution to the loss of bioavailable fixed N (Kalvelage et al., 2013; Dalsgaard et al., 2014). Further ocean deoxygenation as well as expansion of the OMZs worldwide could in turn increase the volume of waters in which N-loss takes place (Stramma et al., 2010; Deutsch et al., 2011), thereby intensifying N limitation of primary production and reducing ocean's ability to sequester atmospheric CO_2 (Falkowski, 1997).

Recent observations have shown the important role of mesoscale processes in the distribution of hydrographic and biogeochemical properties of the ETSP (Stramma et al., 2013; 2014; Bourbonnais et al., 2015; Löscher et al., 2015a; Thomsen et al., 2015). Along the Peruvian coast, instabilities of the main current flow lead to the formation of nonlinear mesoscale eddies which propagate offshore from the site of formation, significantly contributing to the cross-shelf transport of heat, mass, momentum and biogeochemical properties (Chelton et al., 2007; Chaigneau et al., 2008). Likewise, offshore propagation of mesoscale eddies has been shown to increase the spatial extent of the high productivity area of the coastal upwelling (Correa-Ramirez et al., 2007; Chelton et al., 2011), implying their relevance in the export of carbon to the open ocean. Provided that downward transport of organic matter is an essential control of the marine N cycle (Kalvelage et al., 2013), it is of interest to investigate potential changes in N_2O distribution within mesoscale eddies. Although such mesoscale features in the OMZ off Peru have been associated with N-loss processes (Altabet et al., 2012; Stramma et al., 2013), to date no detailed surveys linking mesoscale eddies and N_2O as well as their relevance to N-cycling are available.

The main goal of this study is to present the first set of N_2O measurements collected across three mesoscale eddies which were tracked during the R/V Meteor cruises M90 and M91 in November-December 2012. Furthermore, we use a combination of N_2O concentrations and abundance of selected molecular markers (key genes) for its main formation pathways to elucidate the causes of the observed distribution. Finally, we compare the N_2O concentrations within the center of "young" and "old" mesoscale eddies in order to identify the net effect of their "aging" (offshore propagation).

2 Eddy surveys

The field work was conducted in November-December 2012 during the R/V Meteor cruises M90 and M91, which covered the open ocean and shelf areas off Peru (5°S – 25°S, 75°W – 86°W). Detailed physical and biogeochemical surveys of mesoscale eddies were carried out between 14°S – 18°S and 75°W – 84°W on November 16 to 25 and on December 19 to 23. Based on near-real time satellite data of sea level height anomalies (SSHA) from Aviso (http://aviso.altimetry.fr/), it was possible to identify two mode water (anticyclonic) eddies at the shelf break (eddy A) and the open ocean (eddy B), as well as one cyclonic eddy (eddy C) in the

116 open ocean. Likewise, SSHA data was used to track and revisit eddy A in order to investigate its
117 property's distribution after it started to move westward across the shelf break (Fig. 1).
118
119 ## 2.1 Oceanographic and biogeochemical measurements
120 Ocean velocities were recorded by means of two RDI OceanSurveyor acoustic Doppler current
121 profilers (ADCP), which provided velocity data down to about 700 m and 1200 m depth (75 kHz
122 and 38 kHz, respectively). Discrete water sampling as well as profiling of hydrographic
123 properties was carried out by means of a Sea-Bird CTD/Rosette equipped with 10 L Niskin
124 bottles and double sensors for temperature, conductivity and O_2. Seawater samples for discrete
125 O_2 measurements were collected by drawing bubble-free samples from the CTD/Rosette system.
126 O_2 concentrations of these samples were determined by the Winkler method (Hansen, 1999), and
127 were used to calibrate the O_2 sensors. The overall precision of the O_2 discrete measurements was
128 ±0.45 µmol L^{-1}. Nitrate (NO_3^-), nitrite (NO_2^-) and phosphate (PO_4^{-3}) concentrations were
129 measured on board by means of a QuAAtro auto-analyzer (SEAL Analytical GmbH, Germany)
130 with an overall precision of ±0.1 µmol L^{-1} (NO_3^- and NO_2^-) and ±0.02 µmol L^{-1} (PO_4^{3-}). The N
131 deficit (or N^*) was computed as: $[NO_3^-] + [NO_2^-] - 16 \times [PO_4^{-3}]$. Chlorophyll a (Chl*a*)
132 concentrations were determined by the acetone extraction method followed by fluorometric
133 analysis with a Trilogy® laboratory fluorometer (Welschmeyer, 1994). Turbidity was measured
134 by means of a factory-calibrated Wetlabs Fluorometer/Turbidity sensor with sensitivity up to
135 0.01 NTU (Nephelometric Turbidity Units). Discrete N_2O samples were collected in 22 stations
136 with emphasis on the upper 1000 m of the water column. For this purpose, bubble-free, triplicate
137 samples were collected in 20 mL brown glass flasks and sealed with rubber butyl septa and
138 metallic caps to avoid any gas exchange. Subsequently, a headspace was created on each flask by
139 injecting 10 mL helium (99.999%, AirLiquide GmbH, Düsseldorf, Germany). Microbial activity
140 within the samples was prevented by adding 50 µl of a 1:3 dilution from a saturated mercuric
141 chloride ($HgCl_2$) solution. After an equilibration period of minimum two hours the samples were
142 analyzed using a GC-ECD system (Hewlett Packard (HP) 5890 Series II gas chromatograph).
143 The separation procedure was carried out in a stainless steel column (long: 1.83 m, external
144 diameter: 3.2 mm, internal diameter: 2.2 mm) with a molecular sieve of 5 Å (W.R. Grace & Co.
145 Conn., Columbia, USA). The GC/ECD was calibrated daily by using dilutions of at least three
146 standard gas mixtures up to 10400 ppb (Deuste Steininger GmbH, Mühlheim, Germany).

Standard gases with N_2O < 1000 ppb were calibrated in the department of atmospheric chemistry of the Max-Plank Institute for Biogeochemistry (Jena, Germany) against the NOAA 2006 scale, whereas for N_2O > 1000 ppb the gas molar fraction was determined by means of high-resolution measurements of a calibrated OA-ICOS analyzer (precision better than 0.3 ppb, Arévalo-Martínez, et al., 2013). Calculation of the N_2O concentrations was done as described by Walter et al. (2006). In order to obtain background N_2O concentrations for the ETSP at the time of sampling, we used data from Kock et al. (2015). For this, we computed a mean profile by averaging water column concentrations of N_2O from stations located at the open ocean (86°W section) between 6°S and 16°S. We did not include near-coastal stations for the background profile calculation due to the high variability that can be observed, since this hampers any attempts of obtaining a "typical" profile (see Kock et al., 2015). Our designation of particular stations to eddy cores and edges was based on the SSHA data and follows the criteria defined by Stramma et al. (2013). Eddy core anomalies for oceanographic and biogeochemical parameters were computed as the difference between stations located at or near the center of the eddy and stations outside of it.

2.2 Molecular genetic methods

Nucleic acids samples were collected by filtering up to 1 L of seawater (exact volumes were recorded and the filtration time was lower than 20 min) onto polycarbonate membrane filters with a pore size of 0.2 µm (Millipore). Immediately after collection, samples were frozen at -80 °C until further processing. Nucleic acids were extracted using DNA/RNA AllPrep Kit (Qiagen, Hildesheim, Germany) with additional 15-min cell lysis (10 mg mL^{-1} lysozyme in 10 mM Tris-EDTA, pH 8), and shock freezing in liquid nitrogen before extraction. Quantitative (q)PCR followed protocols in Löscher et al. (2014) except that a ViiA7 qPCR system (Life Technologies, Carlsbad, CA, USA) was used. The sensitivity level for the detection of ammonium monooxygenase (*amoA*) and hydrazine oxidoreductase (*hzo*) genes with this method is 4 copies L^{-1}, whereas for the nitrite reductase (*nirS*) gene is 1 copy L^{-1}.

3 Hydrographic and biogeochemical setting

The properties of the eddies investigated during the M90 (November 2012) and M91 (December 2012) cruises were described in detail by Stramma et al. (2013) and therefore only the main

features are briefly mentioned here. The eddy A was centered at about 16°S, 76°W with the highest intensity (zonal and meridional velocities) in the upper 600 m. As a typical mode water eddy, lifting/deepening of the seasonal/main pycnocline could be observed (McGillicuddy et al., 2007), whereby O_2 was lower, and temperature and salinity were higher in the center of the eddy than at its edges (Fig. 2). Shoaling of the mixed layer depth in the center of the eddy A coincided with a high Chl*a* maximum at about 50 m depth and a up to 30% reduction in O_2 concentrations. The outer western side of cross-shelf sections across eddy A also revealed the influence of coastal upwelling near the shelf break in the upper 180 m. However this feature was detached from the eddy itself as it is shown by temperature, O_2 and velocity distributions (Fig. 2). Meridional velocity distributions as well as temperature, salinity and density fields suggest that eddy A enclosed waters from the Peru-Chile Undercurrent (PCU) at the time of formation near the shelf (Stramma et al., 2013). The eddy B was centered in the open ocean at about 17°S, 83°30'W. Although the velocity distribution was similar to that of eddy A (strong in the upper 600 m), rotational speeds were lower and the temperature, salinity and density anomalies were weaker than in eddy A. Moreover, in comparison with eddy A, the depth of uplifting isopycnals and the mixed layer depth were deeper in eddy B (Fig. 2). As a consequence, the Chl*a* maximum as well as the temperature and O_2 anomalies could be found 100 m deeper in eddy B than in eddy A. A trajectory analysis indicated that eddy B was formed near the shelf about five months before the time of sampling (i.e. 3 months older than eddy A); however a precise location could not be determined with our methods (Stramma et al., 2013). Eddy C was centered in the open ocean at 16°15'S, 80°15'W with maximum velocities at ca. 50 m depth, and a positive density anomaly over the upper 600 m. In contrast to the anticyclonic eddies A and B, temperature and salinity of eddy C were lower and density was higher in the center than in its edges (Fig. 2), although the magnitude of the anomalies was similar to those of eddy A (Stramma et al., 2013). Furthermore, O_2 concentrations were higher in the center of the eddy than in the edges and the size of the O_2 anomaly in the OMZ was larger than for eddy A, indicating ventilation of the OMZ with waters from below the main thermocline. Eddy C was formed at the coast but unlike the anticyclones it moved westward without staying at the shelf (Stramma et al., 2013).

4 Results and discussion

4.1 Depth distribution of N_2O

N_2O concentrations in the water column featured a two-peak structure with maxima N_2O concentrations at the upper and lower boundaries of the OMZ, and depletion at the OMZ's core (Fig. 3). Such pattern has been previously reported for the ETSP (Farías et al., 2007) and similar systems with prominent OMZs (Bange et al., 2001; Bange et al., 2010), and it is generally ascribed to alternating activity of microbial N_2O production/consumption pathways along the vertical O_2 gradients (Codispoti and Christensen, 1985; Ji et al., 2015). Although elevated N_2O concentrations were observed in near-surface waters (up to 88 nmol L^{-1}) of the northwestern edge of eddy A, at the time of sampling the eddy was already detached from the coast and thus these high concentrations could be rather associated to coastal upwelling. In agreement with the distribution of physical properties (Fig. 2), the vertical extent of the low-N_2O waters from the OMZ's core was shifted to shallower depths within the center of mode water eddies A and B. Moreover, shallower minima of N_2O were observed in the upper OMZ for stations located in the center of eddy A (150 m, σ_θ = 26.3 kg m^{-3}) compared to eddy B (250 m, σ_θ = 26.5 kg m^{-3}), whereas in both cases the second N_2O maxima were only slightly displaced towards deeper depths. N_2O concentrations at the boundaries of the OMZ in the center of eddy A were similar to those in its edge, whereas for eddy B the N_2O concentrations in the center were markedly lower than in its edge and outside of it. This is reflected by stronger (negative) N_2O anomalies in eddy B than in eddy A (Fig. 3). Even though the highest velocities for both eddies could be measured until about 600 m depth (σ_θ = 26.7 kg m^{-3}), the O_2, temperature and salinity anomalies in eddy B persisted at deeper depths, which could explain why the N_2O concentrations at the center of eddy B were generally lower through the water column (see Fig. 3 and Fig. S1). The lowest N_2O concentration anomalies were found at the core of the OMZ (defined as the depth range with O_2 < ~ 5 µmol L^{-1}) both at the coastal and open ocean stations (Fig. 3), suggesting enhanced N_2O depletion within the center of eddies A and B.

Recently, Stramma et al. (2013) reported the occurrence of active N-loss processes at the core of the OMZ within the center of both eddies A and B based on the co-occurrence of pronounced NO_2^- maxima as well as O_2 and NO_3^- minima. In their work, Stramma et al. (2013) argued that

nutrient subduction along with reduced productivity might have reduced the flux of organic matter that could fuel N-cycling when the eddies moved towards the open ocean. According to this, a comparatively lower consumption of N_2O by denitrification within the OMZ in center of eddy B should diminish the differences between profiles inside and outside. However, this effect was not visible in the N_2O distribution and conversely, N_2O concentrations were generally lower in the center of eddy B than in the center of eddy A. While depth-integrated N_2O concentration in the OMZ within the open ocean eddy B was only 6% lower than in coastal eddy A, observed differences were as high as 25% when the entire water column (5 m – 1000 m) was considered. Integrated concentrations of O_2 were generally lower in eddy A than in eddy B (37.6±1.7 mol m^{-2} and 46.9±7.2 mol m^{-2}, respectively), suggesting the potential for enhanced N_2O production at the oxic-suboxic boundaries of eddy A (see also section 4.2). However, the extent at which these O_2 concentration differences could explain the observed differences in N_2O concentrations cannot be quantitatively assessed from our data, in particular because of the sampling station density and the fact that we didn't carry out N_2O production rate measurements. Hence, although Stramma et al. (2013) reported a reduction in organic matter turnover for the open ocean eddy B during the M90 cruise, this was not evident for N_2O, which probably reflects either: (1) dissimilarities of the water masses in both eddies at the time of formation (see also 4.3), or (2) slower denitrification rates in the edges of eddy B than in its center. A decreased pace of denitrification could explain the higher N_2O concentration in the OMZ from stations outside of eddy B than those in its center because it would imply slower N_2O consumption (transformation to N_2).

Vertical distribution of N_2O in eddy C was similar to that of the two anticyclonic eddies, with doming of isopycnals in its center causing a shift of the upper and lower N_2O maxima, although in this case towards shallower depths. We found elevated N_2O concentrations at the boundaries of the OMZ and only a slight decrease at 150 m – 400 m depth, where O_2 concentrations fell below 5 µmol L^{-1} (Fig. 3). Nonetheless, N_2O minimum was less pronounced than for eddies A and B at the core of the OMZ, where the strongest (positive) anomalies could be found (Fig. 3). Our results are consistent with the observations of Stramma et al. (2013) who reported elevated O_2 concentrations as well as low NO_2^- accumulation at the center of eddy C, suggesting lower activity of N-loss processes than in eddies A and B. Although upon formation cyclonic eddies

tend to increase subsurface production as mode water eddies do, this effect is not long-lasting and the net downwelling of nutrients ultimately leads to decreased primary productivity (McGillicuddy Jr. et al., 2007). Thus, diminished supply of organic matter which could fuel N-loss within the OMZ's core might have contributed to the relatively higher N_2O concentrations in the OMZ of eddy C than in eddies A and B. Analysis of SSHA data showed, however, that stations assumed to be located in the edge and outside of eddy C were actually influenced by another anticyclonic eddy (see Fig. 1), and therefore are not representative of the mean conditions at the ETSP. Hence, more detailed (higher temporal and spatial resolution) studies of the distribution of N_2O within cyclonic eddies are needed in order to elucidate their role in the water column distribution of this gas in the ETSP.

Both our maximum and minimum of N_2O concentrations along the vertical O_2 gradients were well within the range of previous observations in the ETSP (Farías et al., 2007; 2009; Ryabenko et al., 2012; Kock et al., 2015), and no statistically significant differences (two-sample t-test, p-values > 0.05, $\alpha = 0.05$) were found between our N_2O values at the center of the three eddies and a mean open ocean profile along the 86°W section (Fig. S2). If only stations at about 16°S are considered, however, it can be seen that N_2O depletion at the core of the OMZ was stronger at the center of eddies A and B than outside of them (Fig. S2). Hence, although the influence of eddies on the N_2O distribution in the ETSP as a whole seem to be masked by the high variability of the large-scale distribution of N_2O (see Kock et al., 2015), the negative N_2O anomalies within the core of the OMZ at the center of anticyclonic eddies suggest a locally enhanced sink for this gas.

Given that enhanced concentrations of N_2O can be found within the upper oxycline of the ETSP (e.g. Fig. 3), shoaling of the thermocline within mode water eddies would mean higher N_2O concentrations for a given depth as compared to a background profile. Likewise, coastal upwelling waters off Peru are a known source of extremely high N_2O concentrations to the surface (Arévalo-Martínez et al., 2015). However, since the observed eddies were detached from the coast at the time of sampling, the eddy-driven shoaling of waters with relatively high N_2O concentrations did not contribute to surface fluxes to the atmosphere in this location. In support of this, we observed that even in coastal stations, where a rapid decrease in O_2 concentrations (OMZ start at about 15 m depth) was followed by a narrow peak of N_2O between 10 and 40 m

299 depth (Fig. 3), there wasn't any appreciable variation of N_2O concentrations in the surface.
300 Independent verification of our bottle data derives from surface (~ 6 m) underway measurements
301 performed during the same cruises (Arévalo-Martínez et al., 2015), which also did not show any
302 enhancement of N_2O concentrations during the several cross-eddy sections carried out as part of
303 the M90 and M91 cruises. Hence, although mesoscale eddies seem to influence the vertical
304 distribution of N_2O, they do not have a direct impact on its surface distribution and emissions to
305 the atmosphere since they are "trapped" below the mixed layer.

306

307 ## 4.2 N_2O cycling within coastal eddy A

308 SSHA data from December 2012 indicated that coastal mode water eddy A was still centered
309 near the shelf break at about 16°30'S, 76°30'W. The O_2 distribution along a cross-shelf section
310 between 16°9'S, 76°50'W and 15°23'S, 75°20'W revealed O_2 minima (< 5 µmol L^{-1}) not only in
311 the center of eddy A, but also in the vicinity of the shelf break due to coastal upwelling. (Fig. 4).
312 An intermediate-depth low N_2O layer was consistent with the location of these low-O_2 waters
313 and it reached its maximum extension (70 m – 400 m depth) close to the western side of eddy A
314 center. Although a strong maximum of N_2O (up to 80 nmol L^{-1}) could be observed at about 40 m
315 depth within the station located in the center of the eddy, the subsequent and sharp decrease in
316 O_2 concentrations led to a marked decrease in N_2O.

317 The observed NO_3^- and N^* minima, as well as the pronounced secondary nitrite maximum
318 (Codispoti and Packard, 1980) were consistent with the N_2O distribution, suggesting the
319 occurrence of N-loss processes, particularly in the center of eddy A. Abundances of the *hzo* gene
320 (encoding for hydrazine oxidoreductase), the functional gene marker for anaerobic ammonium
321 oxidation (anammox) (Schmid et al., 2008), were generally higher through the water column
322 within the center of eddy A, with a maximum at about 50 m – 200 m depth (i.e. shallower than
323 outside of the eddy, see Fig. 5). Although anammox does not reflect N_2O consumption, it does
324 provide an indication of active N-loss within the OMZ of the eddy at the time of sampling
325 (Dalsgaard et al., 2012; De Brabandere et al., 2014), which is in line with the observations from
326 previous studies in the ETSP (Altabet et al. (2012); Stramma et al. (2013); Bourbonnais et al.,
327 2015).

Nitrification, as indicated by the depth distribution of gene abundances of *amoA*, the functional key gene for archaeal ammonium oxidation (Rotthauwe et al., 1997), was observed within eddy A, and was stronger in the upper 200 m for the center of the eddy, whereas below 200 m it was of similar magnitude for stations outside and in the center (Fig. 5). This would explain the comparatively high, shallow-depth maximum of N_2O within the center of eddy A (Fig. 4). N_2O production by archaeal ammonia oxidation has been previously been identified to be important in subsurface waters in the ETSP (Löscher et al., 2012). The deeper N_2O maximum, however, cannot be explained by nitrification alone as e.g. Kalvelage et al. (2011) showed a decrease of nitrification rates below the upper oxycline. Furthermore, the linear correlation of ΔN_2O/AOU, which is indicative for nitrification (Nevison et al., 2003), is not present in that depth range and geochemical tracer studies suggest a mixed N_2O production from nitrification and denitrification. (Löscher et al., 2012; Ryabenko et al., 2012).

Based on the structure of the vertical profiles of *amoA* and *nirS* gene abundances, we could also infer that N_2O maxima at the boundaries of the OMZ resulted not only from nitrification but also partially from production during early stages of denitrification. Our observations support the results of Castro-González and Farías (2004), who used N_2O production experiments in the ETSP to show that denitrifiers produce increasing N_2O:N_2 ratios as the O_2 concentrations increase due to the well-known sensitivity of the N_2O reductase to O_2 (Dalsgaard et al., 2014). In order to roughly estimate of the N_2O:N_2 ratios in the upper oxycline of eddy A, we used the observed N_2O concentrations and N^* as an indicator of N-loss. As a result we found that, for example, within the center of the eddy A there was a three-fold increase in the N_2O:N_2 ratio for an O_2 concentration decrease of about 85% (229.1 µmol L^{-1} at 20 m to 32.36 µmol L^{-1} at 50). A similar pattern was observed for stations located outside of the eddy, although the ratios were slightly higher due to the generally higher N_2O concentrations (Fig. 5). Furthermore, we also observed that in the upper 600 m depth the potential for N_2O production via partial denitrification (as inferred from *nirS* abundances) was higher in the center of the eddy than outside (Fig. 5). Nevertheless, within the OMZ's core it was evident that N_2O consumption was stronger in the center of the eddy, suggesting that even though the genes for N_2O production by denitrification were present, they were probably inhibited due to further low O_2 concentrations (~ 3 µmol L^{-1}). It is also likely, however, that under denitrifying conditions N_2O depletion occurs at

a faster rate than production, masking the N_2O production signal. Elevated NO_2^- concentrations (11 μmol L^{-1}) along with close to detection limit NO_3^- concentrations in the OMZ further suggests that complete -and more intense- denitrification took place in the OMZ core at the eddy center (Codispoti and Christensen, 1985; Codispoti et al., 1986). Thus, in general, in the center of the eddy a higher N_2O maxima at the upper boundary of the OMZ resulted from enhanced nitrification and partial denitrification, whereas stronger N_2O depletion at the OMZ's core resulted from enhanced, complete denitrification. Although at depths below 600 m both *amoA* and *nirS* gene abundances were higher outside of the eddy, N_2O concentrations remained similar to those in the center and O_2 was still lower in the eddy's center (Fig. 5). Nevertheless, vertical profiles of the same eddy one month before showed that N_2O concentrations below 600 m were higher in the center (cf. Fig. 3). Thus, it could be that increasing variability beneath the lower boundary of the OMZ was caused by decreasing intensity (velocity) of the eddy below 600 m (Fig. 2). Overall, the net effect of anticyclonic eddy A was an enhancement of N-loss processes within its center, thereby making the OMZ's core an even stronger sink for N_2O than it would be under "mean" conditions.

4.3 Effect of eddy "aging" on N_2O

Westward propagation of mesoscale eddies implies that properties of the waters which were "enclosed" within its center at the time of formation are transported offshore (Chelton et al., 2007). Gruber et al. (2011), for example, suggested that this transport leads to a net reduction of primary productivity in coastal upwelling regions due to nutrient subduction and advection. Since the export of organic matter is the most important factor fueling the N-cycling in the OMZ (Capone and Hutchins, 2013; Babbin et al., 2014), changes in the distribution of the main production/consumption pathways of N_2O are likely to occur under the influence of mesoscale eddies along their transit to open waters. On the following we compare the vertical distributions of N_2O and relevant biogeochemical parameters within the center of the "young" coastal eddy A during the M90 cruise, and the "old" open ocean eddy B. Likewise, we include data of a second survey of eddy A during the M91 cruise (hereafter eddy A-M91). For the comparison we focus on the upper 600 m of the water column since the largest physical and biogeochemical anomalies were observed at this depth range (see Stramma et al., 2013). The cyclonic eddy C is not considered for this analysis given its relatively minor importance for N-loss processes.

Figure 6 depicts the vertical distribution of N_2O from stations located at or nearby the center of the eddies A, B and A-M91. As it can be seen, despite the pronounced N_2O maxima at the upper and lower oxyclines in eddy A-M91, in general, the N_2O concentrations within this eddy were lower than in eddy A and eddy B. Integrated concentration of N_2O within the center of the eddy A was 24% higher than in eddy B (Table 1). This difference can be partially attributed to the fact the N-cycling processes tend to decrease after subsurface nutrients are consumed and/or subducted, and primary production progressively decreases towards the open ocean. This is supported by higher O_2 and NO_3^- concentrations in eddy B than in eddy A, as well as the comparatively lower NO_2^- concentrations in eddy B, which suggests an overall decrease in organic matter respiration in the open ocean eddy. Although the examination of temperature-salinity plots from both cruises suggests the presence of a single water mass within the OMZ of eddies A and B (Fig. S3), with our methods it was not possible to determine the exact time and location of formation of both eddies. Thus, it cannot be ruled out that the differences in the biogeochemical conditions at the time of formation also contributed to the observed differences in N_2O. In a recent study, Thomsen et al. (2015) showed that the eddy-induced transport of shelf-break waters to the open ocean might be an important mechanism for the advection of N-deficient waters away from the coastal area off Peru. Hence, even though the physical properties of both eddies (A and B) are reflected in the vertical distribution of N_2O, the extent at which the observed differences in N_2O concentrations are the result of either decaying N-cycling or the properties of the water masses at the time of formation remains an open question.

In comparison with the eddy A-M91, the integrated concentration of N_2O in the center of eddy A was 53% higher (Table 1). This marked decrease of N_2O in the coastal mode water eddy A only one month after the first sampling points towards an enhancement of N-loss processes within the OMZ of this eddy. In agreement with this observation, eddy A-M91 featured the lowest O_2 and NO_3^- content, as well as the highest NO_2^- values among the three eddies considered (Table 1). Our observations are also in line with the results of Bourbonnais et al. (2015), who reported the occurrence of intense N-loss (up to ~44 µmol L^{-1}) within in the eddy A, as well as an increase in the vertical expansion of the N-deficient waters in eddy A-M91. A substantial increase in water-column integrated abundances of both *amoA* and *nirS* genes was observed in the center of eddy A-M91 with respect to eddies A and B, reflecting the comparatively higher N_2O concentrations

found at the boundaries of the OMZ (cf. Fig. 6). It seems however, that enhanced N_2O production by nitrification and partial denitrification in eddy A-M91 was outpaced by high N_2O consumption in the core of the OMZ with further decreasing O_2 concentrations, which in turn resulted in values even lower than those of the open ocean eddy B. Furthermore, sharp differences in *hzo* gene abundances among the three eddies, with A-M91 featuring considerably higher values (Table 1), put in evidence that N-loss activities in the ETSP were comparatively stronger in coastal eddies at the time of sampling. Likewise this also suggests that strengthening of eddy A (increased velocity) while it stayed stationary on the shelf between the two surveys (M90 and M91) might have led to an N-cycling intensification through the water column.

4.3.1 Changes in N-cycling

In order to provide a quantitative estimate of the amount of denitrification that took place in eddy A, as well as to assess how it changed between the two surveys, in this section we present estimates of nitrate deficit (ΔN) by means of the 'NO' approach (Naqvi and Gupta, 1985). 'NO' is used as a quasi-conservative water mass tracer (Broecker, 1974) and it is defined here as: $[O_2] + 9.1[NO_3^-]$ (Bange et al., 2000). A plot of 'NO' versus potential temperature (θ) from stations located at the center of eddy A during M90 and M91 is shown in Fig. 7. For both cruises we obtained a good correlation between 'NO' and θ after excluding data points from the surface to the upper limit of the OMZ ($O_2 \sim 20$ μmol L^{-1}), as well as those from the OMZ's core ($O_2 < 5$ μmol L^{-1}). Hence, the obtained regression lines ('NO'_{M90}, 'NO'_{M91}, Fig. 7) represent conditions which are expected when the OMZ is not affected by denitrification (Naqvi and Gupta, 1985). We calculated ΔN by using 'NO'_{M90} and 'NO'_{M91} according to the following expression (Bange et al., 2000): $(['NO'_x] - [O_2]) / 9.1 - [NO_3^-] - [NO_2^-]$, where *x* is the corresponding regression line for each cruise.

After integrating ΔN over the depth range of the OMZ, we obtained values of 8.9 mol m^{-2} and 0.02 mol m^{-2} for eddy A during M90 and M91, respectively. ΔN from M90 was significantly higher than most estimates available for a similar OMZ in the Arabian Sea (Naqvi and Gupta, 1985; Howell et al., 1997; Bange et al., 2000), and it was only comparable with values up to 7.3 mol m^{-2} found by Naqvi and Gupta (1985) at about 20°N towards the coast of Oman. ΔN from M91 was however, markedly lower than both ΔN from M90 and ΔN from previous work in the OMZ of the Arabian Sea (minimum ΔN = 1.0 mol m^{-2}; Bange et al., 2000). This suggests not

only strong denitrification activities within mesoscale eddies formed off the Peruvian coast, but also high short-term variability as they move offshore. This results are in agreement with recent work in the ETSP, in which an isotopic approach was used to show the occurrence of intense N-loss by both denitrification and anammox in the OMZ within mesoscale eddies (Bourbonnais et al., 2015). A pronounced Chl*a* and turbidity maximum in the center of eddy A-M91 suggest a potentially increased supply of organic matter which, upon sinking, could stimulate N-loss through anammox and denitrification (Kalvelage et al., 2013; De Brabandere et al., 2014). Therefore it is likely that N-loss still took place in the coastal eddy A during M91, although at rates comparatively lower than those during M90 and the time period elapsed between the two cruises. Our results are in agreement with the work of Löscher et al. (2015), who reported enhanced N_2-fixation rates in the center of mode water eddies, as well as co-occurrence of N_2-fixation and N-loss, suggesting a spatial link between both processes in the ETSP. As part of the same study, Löscher et al. (2015) also found that in general N_2-fixation rates tended to be lower during M91, most likely indicating a decline of biological production during "aging" of the eddy. Hence, although N_2-fixation rates were lower within the mode water eddy A during M91, its occurrence, together with the fact that during M91 we most likely sampled the eddy after a period of intense N-cycling might help to explain the alleviation on the N-deficit between the M90 and 91 cruises. Under the spatial constraints of our survey, one could infer that the N-loss during M91 (as determined both by the N* and 'NO' methods) does not necessarily reflect enhanced denitrification within the eddy at the time of sampling (December), but rather the remaining signal of denitrification during early stages of the eddy which were partially captured when we sampled it in November. However, given that we might have sampled different portions of the eddy despite of a consistent definition of center (i.e. based on SSHA data), a direct comparison remain speculative and further studies employing methods with higher temporal and spatial resolution would be required to assess the temporal variability of N-loss and N_2O consumption in the OMZ of mesoscale eddies.

In order to roughly estimate the amount of N-loss through denitrification which was driven by coastal eddy A between November and December 2012 (27 days), we used our ΔN values and a calculated area of 8.5×10^9 m^2. This resulted in a daily loss flux of 0.04 Tg-N day^{-1}, which if scaled to an annual basis would be comparable with values reported for the Arabian Sea by

Mantoura et al (1993) but lower than most estimates for the same area (Naqvi, 1987; Howell et al., 1997; Bange et al., 2000) and for the eastern tropical South and North Pacific (20-33 Tg-N yr^{-1} and 20-29 Tg-N yr^{-1}, respectively; Codispoti and Richards, 1976; Codispoti and Packard, 1980; DeVries et al., 2012). However, a direct comparison with those studies is not entirely realistic since the mean lifespan of mesoscale eddies off Peru is typically not longer than a few months (Chaigneau, et al., 2008). Therefore the intense N-loss observed within the eddies might represent a transient state which at times contributes significantly to the total N-loss in the ETSP. Since denitrification can also be a source of N_2O (Codispoti and Christensen, 1985; Bakker et al., 2014) we estimated the N_2O production from denitrifying waters within the OMZ's core (O_2 < 5 μmol L^{-1}) of eddy A. For this, we calculated the depth-integrated ΔN_2O ($N_2O_{measured}$ − $N_2O_{equilibrium}$) over the OMZ for both profiles at the center of eddy A (M90 and M91). Using the eddy area and time span between cruises as shown above, we obtained a N_2O daily yield of 1.3×10^{-5} Tg-N_2O day^{-1} (or 8.0×10^{-6} Tg-N day^{-1}). Scaling this value to an annual basis resulted in a N_2O yield of 4.5×10^{-3} Tg-N_2O yr^{-1} (or 2.9×10^{-3} Tg-N yr^{-1}), which is markedly lower than previous values for the Arabian Sea (Mantoura et al 1993; Bange et al., 2001). Accordingly, our estimated N_2O production from denitrification is considerably low in comparison with our estimated denitrification rates from eddy A in November-December 2012 (0.02%), suggesting faster N_2O consumption than production within the OMZ of eddy A for the period of sampling. N_2O production in the OMZ of the Arabian Sea has been reported to amount for at least 2% of the mean denitrification rates (Bange et al, 2001). However this value is not entirely comparable with ours since in that study a whole basin (1.95×10^{12} m^2) is considered and our time span is in the order of months rather than years. It should be pointed out that our denitrification rates and N_2O yields from the OMZ assume a given size and permanence period of the eddy in coastal waters, and moreover, do not take in consideration the progressive decrease in N-loss activities within the eddy center as it moves away from the coast. Therefore, our values are only contentious and are meant to highlight the need of combined biogeochemical-physical studies which account for the annual variability in occurrence, abundance and spatial extent of mesoscale anticyclonic eddies off Peru, given their importance for N-loss processes.

The coastal eddy A was formed on the shelf about two months before the time of sampling, whereas the open ocean eddy B was formed at least five months before our survey. This hampers

a direct comparison of both mode water eddies, in particular because with our methods it was not possible to determine the exact location where eddy B was formed. Nonetheless, the main physical and biogeochemical features of eddies A and B suggest that, in general, the "aging" of mesoscale eddies tends to decrease N_2O concentrations through the water column in response to reduced supply of material to fuel microbial respiration in the boundaries of the OMZ.

4.4 Synthesis

Aside of the temporal and spatial sampling constrains, our observations allowed us to identify common features of the water column distribution of N_2O that arise from the occurrence of different mesoscale eddies in the ETSP. We showed that the main vertical distribution of N_2O within eddies A, B, and C fits well to the typical open ocean distribution reported by previous work in the same area (Löscher et al., 2012; Ryabenko et al., 2012, Kock et al., 2015). Thus, elevated concentrations of N_2O at the upper and lower boundaries of the OMZ could be attributed to production via nitrification and partial denitrification (as inferred from high *amoA* and *nirS* abundances, respectively), whereas denitrification-driven depletion of N_2O was clearly observed at the core of the OMZ (O_2 ~ < 5 µmol L^{-1}). However, vertical shifting of the OMZ due to isocline displacement within the eddies (both anticyclonic and cyclonic) also led to variation of the position of the maxima and minima in the water column. The upward displacement of oxycline waters with high N_2O concentrations was, nevertheless, detached from surface waters and therefore eddies did not affect the surface concentrations of N_2O. Concentrations of N_2O were generally lower through the water column in anticyclonic eddies, suggesting that they transport highly productive waters trapped at the coast and that bear a high potential for intense N-cycling, as has been also shown by recent studies in the ETSP (Bourbonnais et al., 2015; Thomsen et al., 2015). Likewise, we observed that the vertical expansion of low-O_2 waters within the core of the OMZ (O_2 ~ < 5 µmol L^{-1}) within the center of anticyclonic eddies also resulted in an increased area where N_2O depletion was favored. Hence mesoscale eddies in the ETSP might represent a locally relevant, enhanced sink for N_2O. This observation is in line with previous studies which directly measured N-loss in the same eddies (see e.g. Bourbonnais et al. (2015) and Löscher et al. (2015a)). The fact that OMZ core waters (which act as a sink for N_2O) are transported over long distances offshore, also suggests a potentially higher relevance of these region as a sink for N_2O. Nevertheless, given the extremely high production of N_2O in the ETSP

(Kock et al., 2015) and our current lack of understanding of the overall, long-term impact of mesoscale eddies in the biogeochemistry of N_2O; it is, at this point, difficult to assess how relevant this sink term might be.

5 Summary and Conclusions

In this study we used a combined approach including physical, biogeochemical and molecular methods in order to investigate the distribution of N_2O within mesoscale eddies in the ETSP. Overall, a two-peak structure was observed in vertical profiles of N_2O, indicating the alternation between production and consumption processes as a response to the O_2 gradients through the water column. Our results suggest that N_2O concentrations in the water column were consistent with the main physical features of the mesoscale eddies. Hence, lifting/deepening of the seasonal/main pycnoclines in mode water eddies (A and B) was visible for N_2O, with shoaling of the upper maxima and slight displacement of the lower maxima towards deeper depths. Likewise, doming of isopycnals in the open ocean cyclonic eddy (C) caused a shift of the upper and lower N_2O maxima towards shallower depths. O_2 and nutrient (NO_3^- and NO_2^-) distributions as well as abundances of key gene markers for N_2O production processes showed that the upper and lower oxyclines in the boundaries of the OMZ are net sources of N_2O, producing the two observed maxima which envelop the N_2O-depleted waters in the core of the OMZ. Trapping of highly productive coastal waters in anticyclonic eddies (e.g. eddy A) led to a net enhancement of N-loss processes in its center both through denitrification and anammox, thereby making the OMZ's core an even stronger sink for N_2O than it would be under "mean" conditions. However, the strength of the N-cycling processes decreases during the transit of these eddies out of the shelf, mostly in response to a lower supply of organic matter from surface waters and sinking of nutrients as the eddy collapses. Hence our observations suggest that open ocean mode waters eddies tend to produce less N_2O than coastal ones because the weaker maxima that enclose the OMZ core have an overall bigger impact than the reduced N_2O consumption within the OMZ core. Nevertheless, water properties at the time of formation, as well as the pace at which eddies propagate might significantly alter the N_2O concentrations through the water column. Although depth distribution of N_2O in the center of cyclonic eddy C was similar to eddies A and B, in general the concentrations (both maxima and minima) were higher and its relative importance for

N-loss was negligible. Despite of the observed shoaling of upper isopycnals in both mode water and cyclonic eddies; we did not find any appreciable changes in the surface distribution of N_2O since these features are trapped below the mixed layer.

In conclusion, our survey provides the first insights of N_2O distribution within mesoscale eddies in the ETSP, and points out the importance of multidisciplinary approaches in investigating the rather multifaceted N-cycling in OMZs. However, high complexity of the N_2O production and consumption pathways together with unaccounted temporal and spatial variability, hamper the chances of an objective quantification of the net effect of mesoscale eddies in N_2O for the whole ETSP. Projected future deoxygenation and expansion of OMZs has been suggested to significantly increase marine N_2O production. However, an increased strength of the N_2O sink within the core of low-O_2 waters in mesoscale eddies might also play an important role which has not been yet quantified. Hence, it is critical to understand how these prominent features of the circulation might affect N_2O distribution and concentrations in order to be able to assess the variability of its sources and sinks strength.

Author contribution

L.S., D.L.A.-M, and H.W.B. conceived the study; D.L.A.-M. set up the instrumentation for discrete N_2O measurements on board of the R/V Meteor and carried out the field work together with A.K. and H.W.B.. D.L.A.-M. and A.K. processed and calibrated depth profile N_2O data. C.R.L. collected and processed the molecular data. L.S. processed and analyzed hydrographic data. D.L.A.-M. wrote the manuscript with contributions from H.W.B., A.K., C.R.L., R.A.S., and L.S.

Acknowledgements

This study was funded by the DFG-supported project SFB754 (http://www.sfb754.de), the BMBF joint project SOPRAN II and III (FKZ 03F0611A and FKZ 03F662A), and the EU FP7 project InGOS (Grant Agreement # 284274). We thank the Peruvian authorities for authorizing us to conduct the study in their territorial waters. We also would like to thank our Peruvian colleagues from IMARPE (M. Graco, A. Bernal, G. Flores and V. León) for their logistical support. We thank the captains and crew of the R/V Meteor for their assistance during the cruises M90 and M91. Likewise, we thank T. Baustian, A. Bernal, J. Craig, G. Eirund, G. Flores, V.

León, M. Lohmann, N. Martogli, K. Nachtigall and G. Krahmann for their contributions to the processing of the different data sets. The altimeter data used for Fig. 1 were produced by Ssalto/Duacs and distributed by Aviso with support from Cnes.

References

Altabet, M. A., Ryabenko, E., Stramma, L., Wallace, D. W. R., Frank, M., Grasse, P., and Lavik, G.: An eddy-stimulated hotspot for fixed nitrogen-loss from the Peru oxygen minimum zone, Biogeosciences, 9, 4897–4908, 2012.

Arévalo-Martínez, D. L., Beyer, M., Krumbholz, M., Piler, I., Kock, A., Steinhoff, T., Körtzinger, A., and Bange, H. W.: A new method for continuous measurements of oceanic and atmospheric N_2O, CO and CO_2: performance of off-axis integrated cavity output spectroscopy (OA-ICOS) coupled to non-dispersive infrared detection (NDIR), Ocean Sci., 9, 1071–1087, 2013.

Arévalo-Martínez, D. L., Kock, A., Löscher, C. R., Schmitz, R. A., and Bange, H. W.: Massive nitrous oxide emissions from the tropical South Pacific Ocean, Nature Geosci., 8, 530–533, doi:10.1038/ngeo2469, 2015.

Babbin, A., R., Keil, R. G., Devol, A. H., and Ward, B.: Organic matter stoichiometry, flux, and oxygen control nitrogen loss in the ocean, Science, 344, 406 – 408, 2014.

Bakker, D. C. E., Bange, H. W., Gruber, N., Johannenssen, T., Upsill-Goddard, R. C., Borges, A. V., Delille, B., Löscher, C. R., Naqvi, S. W. A., Omar, A. O., and Santana-Casiano, J. M.: Air-sea interactions of natural long-lived greenhouse gases (CO_2, N_2O, CH_4) in a changing climate, in: Ocean-atmosphere interactions of gases and particles, Liss, P. S., and Johnson, M. T. (eds.), 113–169, Springer, Heidelberg, 2014.

Bange, H. W., Rixen, T., Johansen, A. M., Siefert, R. L., Ramesh, R., Ittekkot, V., Hoffmann, M. R., and Andreae, M. O.: A revised nitrogen budget for the Arabian Sea, Global Biogeochem. Cycles, 14(4), 1283–1297, 2000.

Bange, H. W., Rapsomanikis, S., and Andreae, M. O.: Nitrous oxide cycling in the Arabian Sea, J. Geophys. Res., 106(C1), 1053–1065, 2001.

624 Bange, H. W., Freing, A., Kock, A., and Löscher, C. R.: Marine pathways to nitrous oxide, in:
625 Nitrous oxide and climate change, Smith, K. (ed.), 36–62, Earthscan, London, 2010.

626 Bourbonnais, A., Altabet, M. A., Charoenpong, C. N., Larkum, J., Hu, H., Bange, H. W., and
627 Stramma, L.: N-loss isotope effects in the Peru oxygen minimum zone studied using a mesoscale
628 eddy as a natural tracer experiment, Global. Biogeochem. Cycles, 29,
629 doi:10.1002/2014GB005001, 2015.

630 Broecker, W. S.: "NO", a conservative water-mass tracer, Earth Planet. Sci. Lett., 23, 100–107,
631 1974.

632 De Brabandere, L., Canfield, D. E., Dalsgaard, T., Friederich, G. E., Revsbech, N. P., Ulloa, O.,
633 and Thamdrup, B.: Vertical partitioning of nitrogen-loss processes across the oxic-anoxic
634 interface of an oceanic oxygen minimum zone, Environ. Microbiol., 16(10), 3041–3054, 2014.

635 DeVries, T., Deutsch, C., Primeau, F., Chang, B., and Devol, A.: Global rates of water-column
636 denitrification derived from nitrogen gas measurements, Nature Geosci., 5, 547–550, 2012.

637 Capone, D. G., and Hutchins, D. A.: Microbial biogeochemistry of coastal upwelling regimes in
638 a changing ocean, Nature Geosci., 6, 711–717, 2013.

639 Castro-González, M., and Farías, L.: N_2O cycling at the core of the oxygen minimum zone off
640 northern Chile, Mar. Ecol. Prog. Ser., 280, 1–11, 2004.

641 Chaigneau, A., Gizolme, A., and Grados, C.: Mesoscale eddies off Peru in altimeter records:
642 Identification algorithms and eddy spatio-temporal patterns, Prog. Oceanogr., 79, 106–119,
643 2008.

644 Chelton, D. B., Schlax, M. G., Samelson, R. M., and de Szoeke, R. A.: Global observations of
645 large oceanic eddies, Geophys. Res. Lett., 34, L15606, doi:10.1029/2007GL030812, 2007.

646 Chelton, D. B., Gaube, P., Schlax, M. G., Early, J. J., and Samelson, R. M.: The influence of
647 nonlinear mesoscale eddies on near-surface oceanic chlorophyll, Science, 334, 328–332, 2011.

648 Codispoti, L. A.: Interesting times for marine N_2O, Science, 327, 1339–1340, 2010.

649 Codispoti, L. A., and Christensen, J. P.: Nitrification, denitrification and nitrous oxide cycling in
650 the eastern tropical South Pacific Ocean, Mar. Chem., 16, 277–300, 1985.

651 Codispoti, L. A., and Packard, T. T.: Denitrification rates in the eastern tropical South Pacific, J.
652 Mar. Res., 38, 453–477, 1980.

653 Codispoti, L. A., and Richards, F. A.: An analysis of the horizontal regime of denitrification in
654 the eastern tropical North Pacific, Limnol. Oceanogr., 21(3), 379–388, 1976.

655 Codispoti, L. A., Friederich, G. E., Packard, T. T., Glover, H. E., Kelly, P. J., Spinrad, R. W.,
656 Barber, R. T., Elkins, J., W., Ward, B. B., Lipschultz. F., and Lostaunau, N.: High nitrite levels
657 off northern Peru: a signal of instability in the marine denitrification rate, Science, 233, 1200–
658 1202, 1986.

659 Correa-Ramirez, M. A., Hormazábal, S., and Yuras, G.: Mesoscale eddies and high chlorophyll
660 concentrations off central Chile (29°–29°S), Geophys. Res. Lett., 34, L12604, doi:
661 10.1029/2007GL029541, 2007.

662 Dalsgaard, T., Thamdrup, B., Farías, L., and Revsbech, N. P.: Anammox and denitrification in
663 the oxygen minimum zone of the eastern South Pacific, Limnol. Oceanogr., 57(5), 1331–1346,
664 2012.

665 Dalsgaard, T. Stewart, F. J., Thamdrup, B., De Brabandere, L., Revsbech, N. P., Ulloa, O.,
666 Canfield, D. E., and DeLong, E. F.: Oxygen at nanomolar levels reversibly suppresses process
667 rates and gene expression in anammox and denitrification in the oxygen minimum zone off
668 northern Chile, mBio, 5(6), e01966–14. doi:10.1128/mBio.01966–14, 2014.

669 Deutsch, C., Brix, H., Ito, T., Frenzel, H., and Thompson, L.: Climate-forced variability of ocean
670 hypoxia, Science, 333, 336–339, 2011.

671 Falkowski, P. G.: Evolution of the nitrogen cycle and its influence on the biological
672 sequestration of CO_2 in the ocean, Nature, 387, 272–275, 1997.

673 Farías, L., Paulmier, A., and Gallegos, M.: Nitrous oxide and N-nutrient cycling in the oxygen
674 minimum zone off northern Chile, Deep-Sea Res. Part I, 54, 164–180, 2007.

675 Farías, L., Castro-González, M., Cornejo, M., Charpentier, J., Faúndez, J., Boontanon, N., and
676 Yoshida, N.: Denitrification and nitrous oxide cycling within the upper oxycline of the eastern
677 tropical South Pacific oxygen minimum zone, Limnol. Oceanogr., 54(1), 132–144, 2009.

678 Goreau, T. J., Kaplan, W. A., Wofsky, S. C., McElroy, M. B., Valois, F. W., and Watson, S. W.:
679 Production of NO_2^- and N_2O by nitrifying bacteria at reduced concentrations of oxygen, Appl.
680 Environ. Microb., 40(3), 526–532, 1980.

681 Gruber, N., Lachkar, Z., Frenzel, H., Marchesiello, P., Münnich, M., McWilliams, J. C., Nagai,
682 T., and Plattner, G.-K.: Eddy-induced reduction of biological production in eastern boundary
683 upwelling systems, Nature Geosci., 4, 787–792, 2011.

684 Hansen, H. P.: Determination of oxygen, in: Methods of Seawater Analysis, Grasshoff, K. G.,
685 Kremling, K., and Ehrhardt, M. (eds.), Wiley-VCH, Weinheim, 75–90, 1999.

686 Howell, E. A., Doney, S. C., Fine, R. A., and Olson, D. B.: Geochemical estimates of
687 denitrification in the Arabian Sea and the Bay of Bengal during WOCE, Geophys. Res. Lett., 24,
688 2549–2552, 1997.

689 Ji, Q., Babbin, A. R., Jayakumar, A., Oleynik, S., and Ward, B.: Nitrous oxide production by
690 nitrification and denitrification in the Eastern Tropical South Pacific oxygen minimum zone,
691 Geophys. Res. Lett., 42, doi:10.1002/2015GL066853, 2015.

692 Kalvelage, T., Jensen, M. M., Contreras, S., Revsbech, N. S., Lam, P., Günter, M., LaRoche, J.,
693 Lavik, G., and Kuypers, M. M. M.: Oxygen sensitivity of anammox and coupled N-cycle
694 processes in the oxygen minimum zones, PloS ONE, 6(12), e29299,
695 doi:10.1371/journal.pone.0029299, 2011.

696 Kalvelage, T., Lavik, G., Lam, P., Contreras, S., Arteaga, L., Löscher, C. R., Oschlies, A.,
697 Paulmier, A., Stramma, L., and Kuypers, M. M. M.: Nitrogen cycling driven by organic matter
698 export in the South Pacific oxygen minimum zone, Nature Geosci., 6, 228–234, 2013.

699 Karstensen, J., Stramma, L., and Visbeck, M.: Oxygen minimum zones in the eastern tropical
700 Atlantic and Pacific oceans, Prog. Oceanogr., 77, 331–350, 2008.

701 Kock, A., Arévalo-Martínez, D. L., Löscher, C. R., and Bange, H. W.: Differences between
702 coastal and open ocean distributions of N_2O in the oxygen minimum zone off Peru,
703 Biogeosciences Discuss., 12, 10167-10193, 2015.

Löscher, C. R., Kock, A., Könneke, M., LaRoche, J., Bange, H. W., and Schmitz, R. A.: Production of oceanic nitrous oxide by ammonia-oxidizing archaea, Biogeosciences, 9, 2419–2429, 2012.

Löscher, C. R., Großkopf, T., Desai, F. D., Gill, D., Schunck, H., Croot, P. L., Schlosser, C., Neulinger, S. C., Pinnow, N., Lavik, G., Kuypers, M. M. M., LaRoche, J., and Schmitz, R. A.: Facets of diazotrophy in the oxygen minimum zone waters off Peru, The ISME Journal, 8, 2180–2192, 2014.

Löscher C. R., Bourbonnais, A., Dekaezemacker, J., Charoenpong, C. N., Altabet, M. A., Bange, H. W., Czeschel, R., Hoffmann, C., and Schmitz, R. A.: N_2 fixation in eddies of the eastern tropical South Pacific Ocean, Biogeosciences Discuss., 12, 18945–18972, 2015a.

Löscher, C. R., Bange, H. W., Schmitz, R. A., Callbeck, C. M., Engel, A., Hauss, H., Kanzow, T., Kiko, R., Lavik, G., Loginova, A., Melzner, F., Neulinger, S. C., Pahlow, M., Riebesell, U., Schunck, H., Thomsen, S., and Wagner, H.: Water column biogeochemistry of oxygen minimum zones in the eastern tropical North Atlantic and eastern tropical South Pacific Oceans, Biogeosciences Discuss., 12, 4495–4556, 2015b.

McGillicuddy Jr., D. J., Anderson, L. A., Bates, N. R., Bibby, T., Buesseler, K. O., Carlson, C. A., Davis, C. S., Ewart, C., Falkowski, P. G., Goldthwait, S. A., Hansell, D. A., Jenkins, W. J., Johnson, R., Kosnyrev, V. K., Ledwell, J. R., Li, Q. P., Siegel, D. A., and Steinberg, D. K.: Eddy/wind interactions stimulate extraordinary mid-ocean plankton blooms, Science, 316, 1021–1026, 2007.

Mantoura, R. F. C., Law, C. S., Owens, N. J. P., Burkill, P. H., Woodward, E. M. S., Howland, R. J. M., and Llewellyn, C. A.: Nitrogen biogeochemical cycling in the northwestern Indian Ocean. Deep-Sea Res. Part II, 40(3), 651–671, 1993.

Myhre, G. D., Schindell, D., Bréon, F.-M., Collins, W., Fuglestvedt, J., Huang, J., Koch, D., Lamarque, J.-F., Lee, D., Mendoza, B., Nakajima, T., Robock, A., Stephens, G., Takemura, T., and Zhang, H.: Anthropogenic and natural radiative forcing, in: Climate Change 2013: The Physical Science Basis, Contribution of Working Group I to the Fifth Assessment Report of the Intergovernmental Panel on Climate Change, Stocker, T. F., Qin, D., Plattner, G.-K., Tignor, M.,

Allen, S. K., Boschung, J., Nauels, A., Xia, Y., Bex, V., and Midgley, P. M. (eds.), Cambridge University Press, Cambridge, United Kingdom and New York, USA, 129–234, 2013.

Naqvi, S. W. A.: Some aspects of the oxygen-deficient conditions and denitrification in the Arabian Sea, J. Mar. Res., 45, 1049–1072, 1987.

Naqvi, S. W. A., and Gupta, R. S.: 'NO', a useful tool for the estimation of nitrate deficits in the Arabian Sea, Deep-Sea. Res., 32(6), 665–674, 1985.

Naqvi, S. W. A., Bange, H. W., Farias, L., Monteiro, P. M. S., Scranton, M. I., and Zhang, J.: Marine hypoxia/anoxia as a source of CH_4 and N_2O, Biogeosciences, 7, 2159–2190, 2010.

Nevison, C. D., Butler, J. H., and Elkins, J. W: Global distribution of N_2O and the ΔN_2O-AOU yield in the subsurface ocean, Global Biogeochem. Cycles, 17(4), 1119, doi:10.1029/2003GB002068, 2003.

Paulmier, A., Ruiz-Pino, D., and Garcon, V.: The oxygen minimum zone (OMZ) off Chile as an intense source of CO_2 and N_2O, Cont. Shelf. Res., 28, 2746–2756, 2008.

Ravishankara, A. R., Daniel, J. S., and Portmann, R. W.: Nitrous oxide (N_2O): The dominant ozone-depleting substance emitted in the 21st Century, Science, 326, 123–125, 2009.

Rotthauwe, J. H., Witzel, K. P., and Liesack, W.: The ammonia monooxygenase structural gene *amoA* as a functional marker: molecular fine-scale analysis of natural ammonia-oxidizing populations. Appl. Environ. Microbiol., 63(12), 4704 – 4712,1997.

Ryabenko, E., Kock, A., Bange, H. W., Altabet, M. A., and Wallace, D. W. R.: Contrasting biogeochemistry of nitrogen in the Atlantic and Pacific Oxygen Minimum Zones, Biogeosciences, 9, 203–215, 2012.

Schmid, M. C., Hooper, A. B., Klotz, M. G., Woebken, D., Lam, P., Kuypers, M. M. M., Pommerening-Roeser, A., Op den Camp, H. J. M., and Jetten, M. S. M.: Environmental detection of octahaem cytochrome c hydroxylamine/hydrazine oxidoreductase genes of aerobic and anaerobic ammonium-oxidizing bacteria, Environ. Microbiol., 10(11), 3140–3149, 2008.

Stramma, L., Schmidtko, S., Levin, L. A., and Johnson, G. C.: Ocean oxygen minima expansions and their biological impacts, Deep-Sea Res. Part I, 57, 587–595, 2010.

759 Stramma, L., Bange, H. W., Czeschel, R., Lorenzo, A., and Frank, M.: On the role of mesoscale
760 eddies for the biological productivity and biogeochemistry in the eastern tropical Pacific Ocean
761 off Peru, Biogeosciences, 10, 7293–7306, 2013.

762 Stramma, L., Weller, R. A., Czeschel, R., and Bigorre, S.: Eddies and an extreme water mass
763 anomaly observed in the eastern south Pacific at the Stratus mooring, J. Geophys. Res. Oceans,
764 119, 1068–1083, 2014.

765 Suntharalingam, P., Sarmiento, J. L., and Toggweiler, J. R.: Global significance of nitrous-oxide
766 production and transport from oceanic low-oxygen zones: a modeling study, Global
767 Biogeochem. Cycles, 14(4), 1353–1370, 2000.

768 Thomsen, S., Kanzow, T., Krahmann, G., Greatbatch, R. J., Dengler, M., and Lavik, G.: The
769 formation of a subsurface anticyclonic eddy in the Peru-Chile Undercurrent and its impact on the
770 near-coastal salinity, oxygen and nutrient distributions, J. Geophys. Res. Oceans, 120,
771 doi:10.1002/2015JC010878, 2015.

772 Walter, S., Breitenbach, U., Bange, H. W., Nausch, G., and Wallace, D. W. R.: Distribution of
773 N_2O in the Baltic Sea during transition from anoxic to oxic conditions, Biogeosciences, 3, 557–
774 570, 2006.

775 Welschmeyer, N.: Fluorometric analysis of Chlorophyll a in the presence of Chlorophyll b and
776 phaeopigments, Limnol. Oceanogr. 39(8), 1985–1992, 1994.

777

778

779

780

781

782

783

784

785

Table 1. Comparison of physical and biogeochemical properties of mode water eddies in the ETSP during the M90 (November 2012) and M91 (December 2012) cruises. [a] Values taken from Stramma et al. (2013) refer to the depth range wherein the strongest anomalies were observed. N_2O, O_2, NO_3^-, NO_2^- and selected functional gene markers are expressed as integrated concentrations/abundances over the water column.

	A (M90)	A(M91)	B(M90)
Vertical extent (m)[a]	0 - 600	0 - 600	0 - 600
Radius (km) [a]	52.0	-	48.8
Volume (10^{12} m^3) [a]	5.2	-	4.7
N_2O (mol m^{-2})	0.034	0.016	0.026
O_2 (mol m^{-2})	36.4	10.8	42.9
NO_3^- (mol m^{-2})	14.8	12.4	15.8
NO_2^- (mol m^{-2})	1.6	2.6	0.52
amoA (10^8 copies m^{-2})	19.54	598.5	379.3
nirS (10^8 copies m^{-2})	0.37	57.9	0.23
hzo (10^8 copies m^{-2})	4.27	101773	2.9

Figures

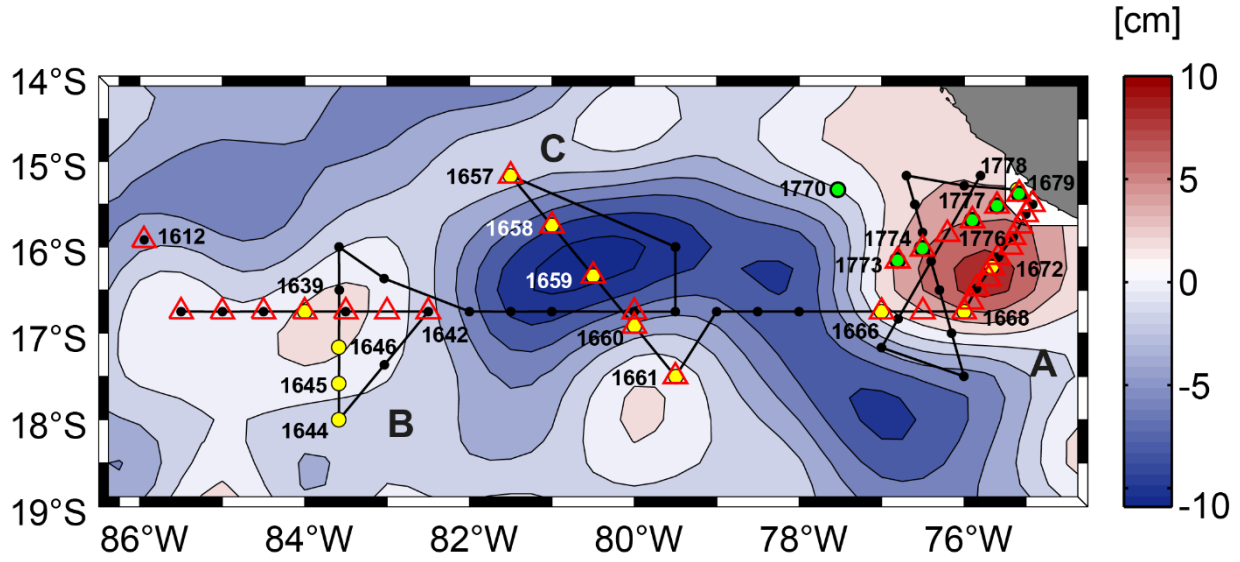

Figure 1. Map of sampling locations in the ETSP. Aviso sea level height anomaly for the 21st of November 2012 is shown (anticyclonic eddies are depicted in red and cyclonic in blue). The cruise track and CTD stations with bottle sampling from the M90 cruise are shown in black. Open triangles indicate the hydrographic stations shown in Fig. 2. Sampling stations within the mode water eddies A and B, as well as the open ocean cyclonic eddy C are highlighted in yellow, whereas the cross-shelf section carried out during the M91 cruise is displayed in green. Station 1770 from the M91 cruise was used for the molecular work shown in Fig.5.

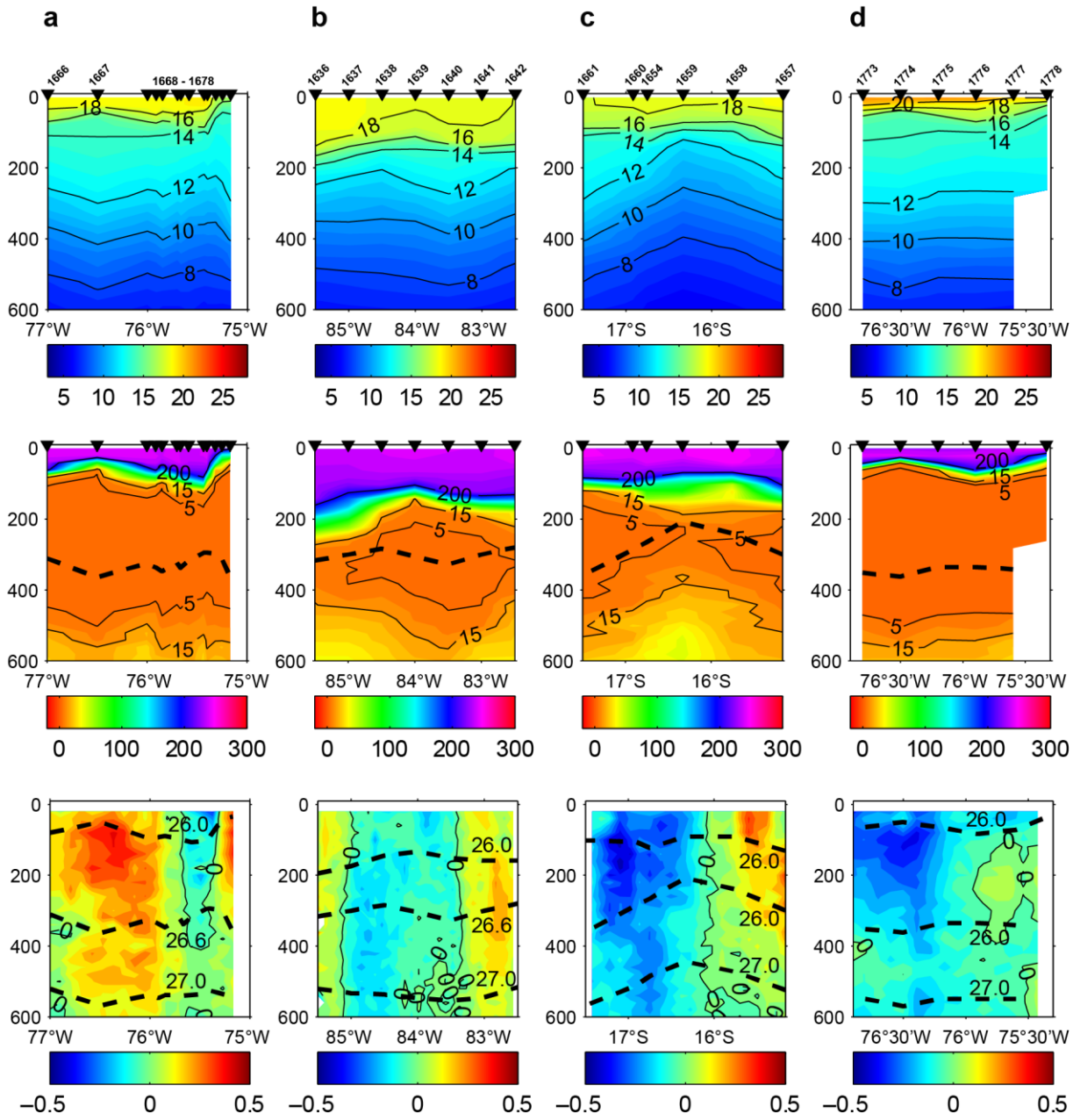

Figure 2. Hydrographic conditions at the time of sampling in the ETSP. Temperature in °C (upper panels), O_2 in µmol kg^{-1} (middle panels) and zonal (a,c,d)/meridional (b) velocity in m s^{-1} (lower panels) for eddies A, B and C during the M90 cruise (November 2012; a-c), as well as for eddy A during the M91 cruise (December 2012; d) are shown. Locations of CTD profiles are marked by black triangles (cf. Fig. 1) and the isopycnal σ_θ=26.6 kg m^{-3} near the core of the OMZ is included in the O_2 sections as a black dashed line. Dashed lines in the velocity plots indicate potential density.

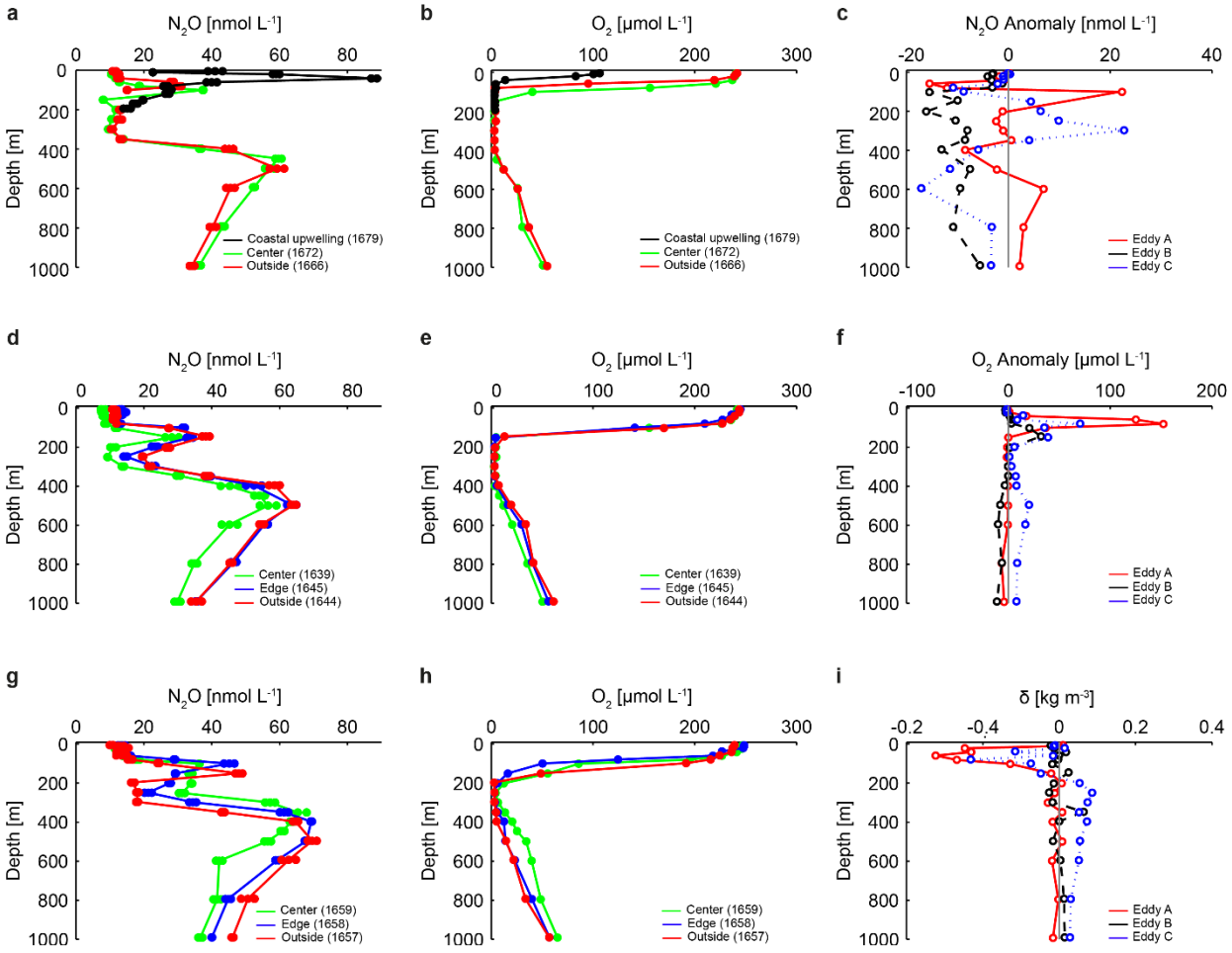

826

827 Figure 3. Vertical of distribution of N_2O and O_2 across the mode water eddies A (a – b), B (d –
828 e), and the cyclonic eddy C (g – h) during the M90 cruise in November 2012. Selected depth
829 profiles of N_2O and O_2 are shown in (a, d, g) and (b, e, h), respectively. Black lines/symbols in
830 (a) and (b) indicate the northwesternmost station of eddy A, in which the influence of coastal
831 upwelling was observed. Numbers in parenthesis indicate the station numbers (cf. Fig. 1). For
832 N_2O the standard deviation from triplicate samples is depicted by circles around the
833 concentration values at each depth. N_2O, O_2 and density (δ) core anomalies for the eddies
834 sampled during M90 are shown in (c), (f), and (i), respectively.

835

836

837

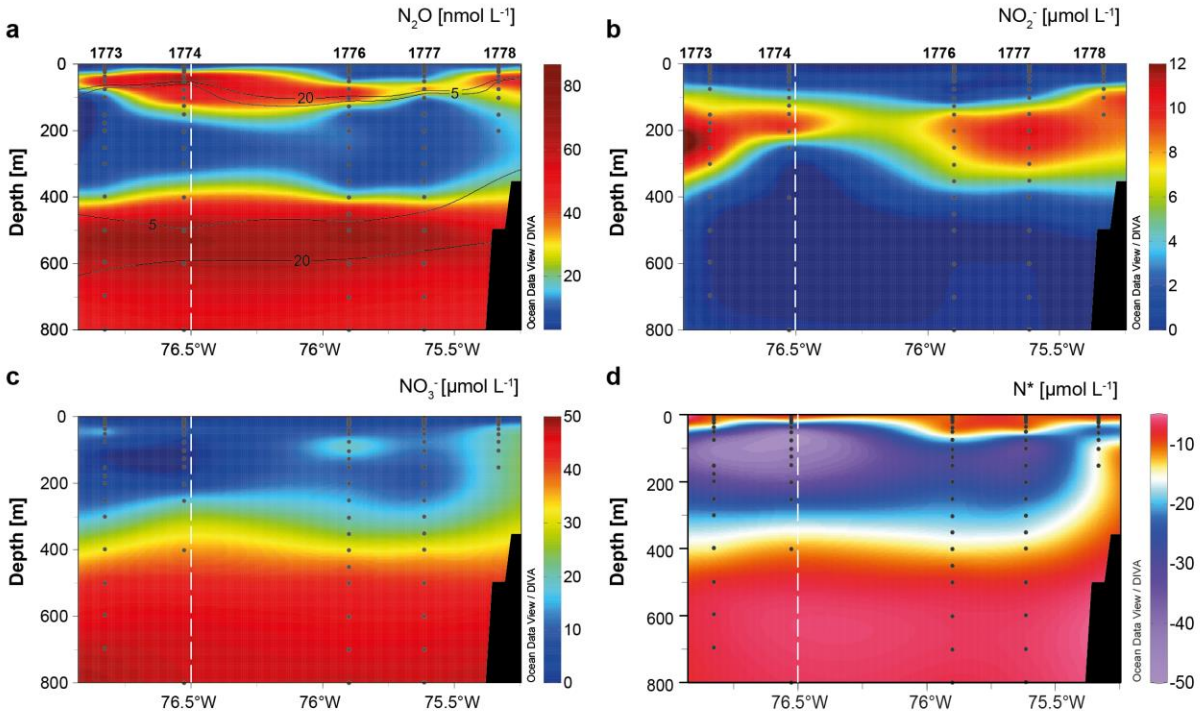

Figure 4. Cross-shelf distribution of N_2O (a), NO_2^- (b), NO_3^- (c) and N^* (d) along eddy A in December 2012 (16.2°S, 76.9°W to 15.3°S 75.2°W, see Fig. 1). Contours in (a) represent O_2 concentrations (in µmol L^{-1}). The white dashed lines indicate the approximate location of the eddy center according to SSHA data. Numbers above panels (a) and (b) are the station numbers (cf. Fig. 1).

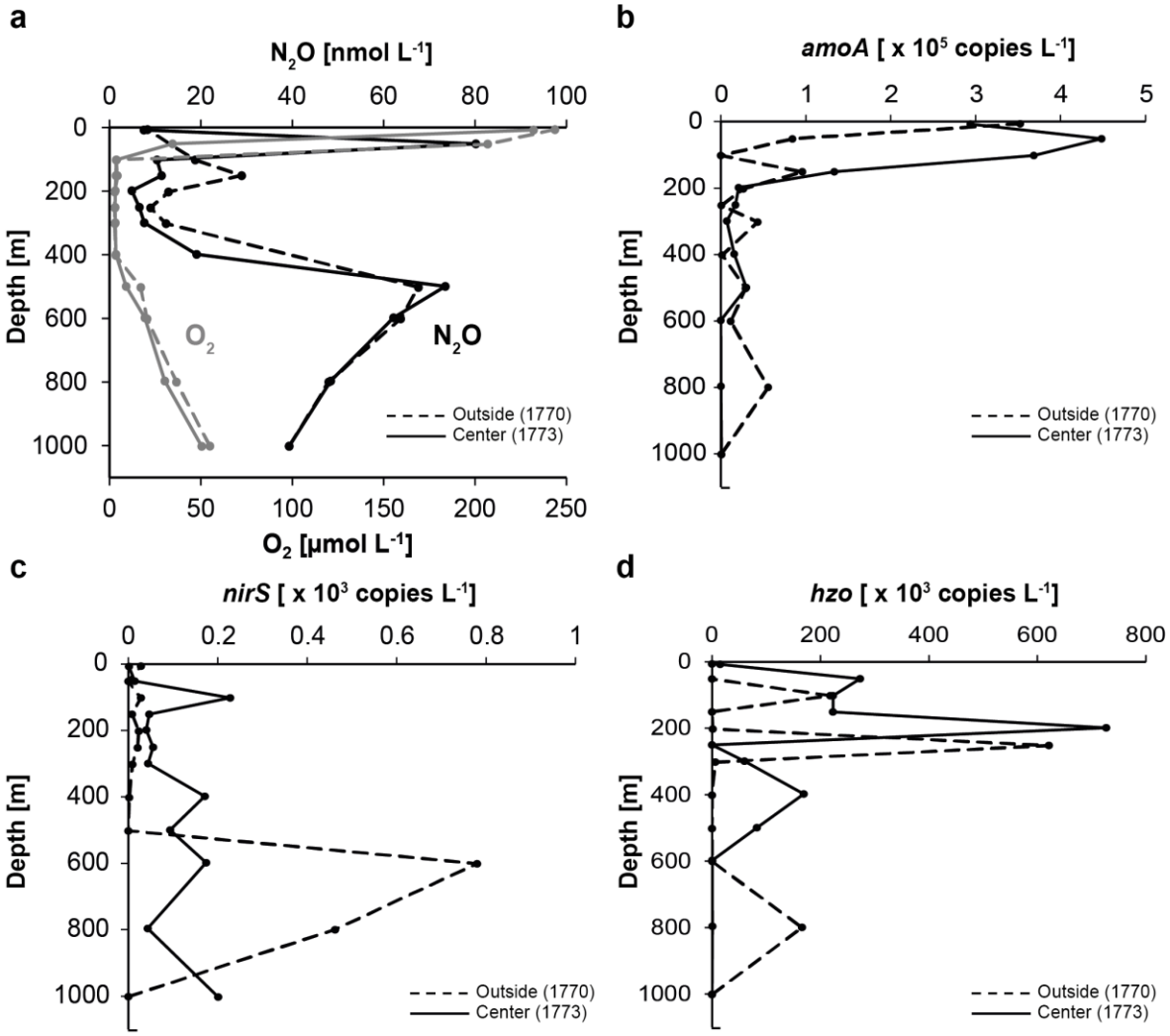

853

854 Figure 5. Vertical distribution of N_2O and O_2 concentrations (a), as well as gene abundance of
855 *amoA* (b), *nirS* (c) and *hzo* (d) within the center (solid lines) and outside (dashed lines) of eddy A
856 in December 2012 (M91 cruise). The numbers in parenthesis indicate the station numbers (cf.
857 Fig. 1).

858

859

860

861

862

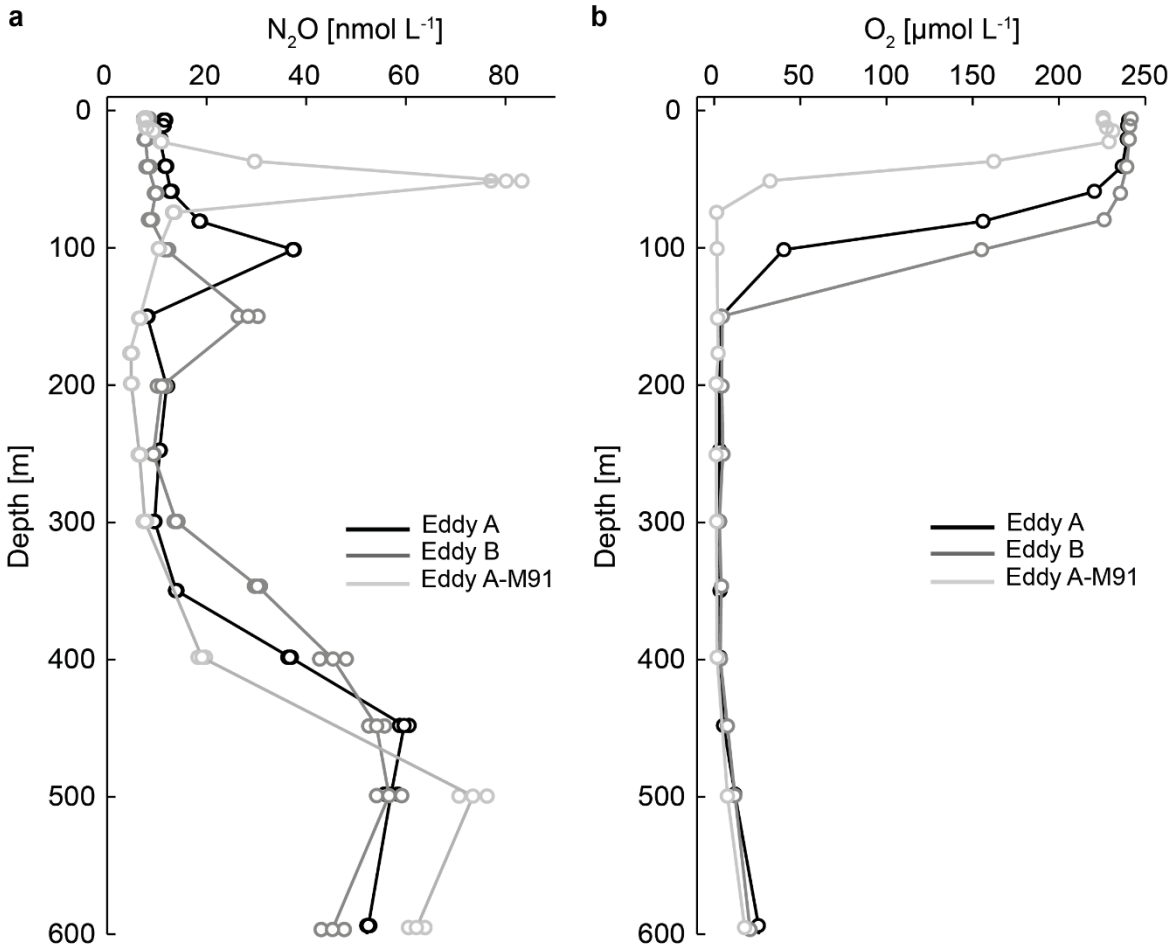

863

864 Figure 6. Vertical distribution of N_2O (a) and O_2 (b) within the center of the anticyclonic eddies
865 A, B and A-M91. For N_2O the standard deviation from triplicate samples is depicted by circles
866 around the concentration values at each depth.

867

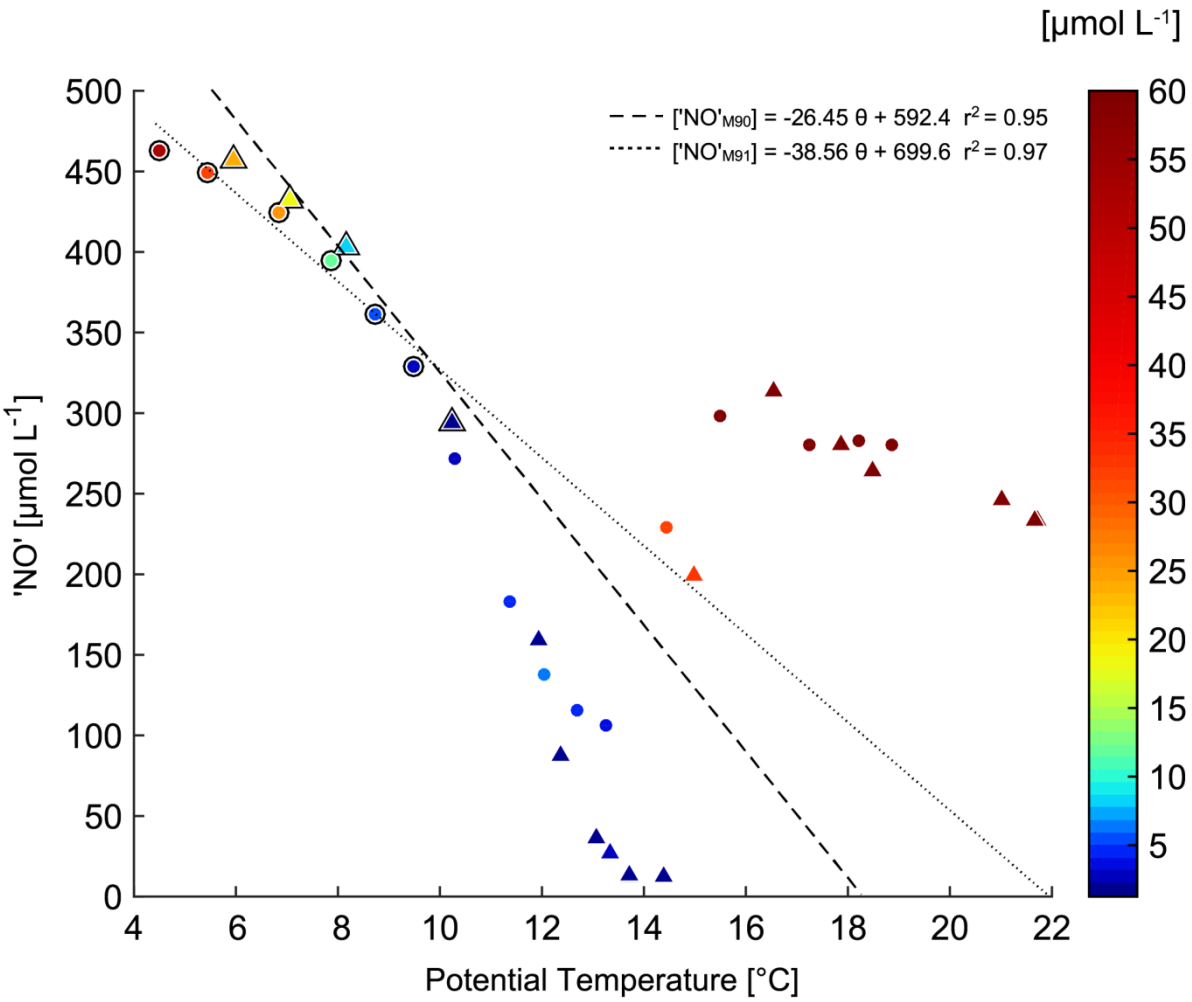

868

869 Figure 7. 'NO' vs. potential temperature (θ) for stations located at the center of eddy A during
870 M90 (November 2012; circles) and M91 (December 2012; triangles). The color bar represents
871 the O_2 concentrations (scale has been truncated at 60 µmol L^{-1}). 'NO' values from non-
872 denitrifying waters (O_2 > 5 µmol L^{-1}) are highlighted in black and were used for the linear least-
873 squares regressions.